Journal of Advances in Science and Engineering 6 (2022) 1 – 12

Journal of Advances in Science and Engineering (JASE)

Journal homepage: www.sciengtexopen.org/index.php/jase

Leaching of Ibute-Nze kaolin iron-oxide impurity with oxalic acid process optimization of dissolution conditions using response surface methodology

Daniel O. Ochi *, Hauwau Mahmud, Marcellinus O. Ani, Salisu O. Aliu

Department of Chemical Engineering, Auchi Polytechnic, Auchi, Edo State, Nigeria

ARTICLE INFO

Article history:
Received 24 February 2022
Received in revised form
21 March 2022
Accepted 23 March 2022
Available online
24 March 2022

Keywords:
Box-Behnken design
Ibute-Nze kaolin clay
Iron oxide removal
Leaching
Oxalic acid
Process optimization

ABSTRACT

The goal of this research was to remove iron oxide from Ibute-Nze kaolin by dissolving the clay mineral in an aqueous oxalic acid solution and optimizing the process. The chemical composition of the raw and modified clay was determined using x-ray fluorescence, and the morphology of the solid sample was determined using a scanning electron microscope. The best conditions for the oxalic acid leaching of iron-oxides impurity from Ibute-Nze kaolin were determined using response surface methodology based on Box-Behnken design. The studies were carried out within the following process parameter ranges: 40–90℃ leaching temperature; 0.075-0.355mm particle size; 1–6 mol/dm^3 acid concentration; 0.02–0.12 g/cm^3 kaolin sample to acid ratio and 30-240 min contact time. The characterization revealed that Ibute-Nze clay is kaolinitic in nature and calcination at 750℃ opens more pores for its leaching. According to the analysis of variance, a second-order polynomial regression equation provided the best fitting for the experimental data. The predicted and experimental response values were shown to be correlated (R^2 = 0.9276) in the experimental runs. The following were found to be the best conditions for the leaching process variables: 83.2051℃ leaching temperature, 0.0827mm particle size, 3.6179mol/dm^3 acid concentration; 0.0287g/cm^3 kaolin to acid ratio and 217.932min reaction time. The chemical leaching process was 92.6035 per cent under these conditions, which made the clay good for industrial applications.

1. Introduction

Kaolin clay is a type of clay made primarily of the mineral kaolinite, which can be found all over the world. It's likewise referred to as white clay or China clay. Kaolin is called after the Kao-ling Hill in China, which has been mining this clay for hundreds of years. Kaolinite is presently mined in several nations, including China, the United States, Brazil, Pakistan, Bulgaria, and others. It grows best on soils created by the weathering of rocks in hot, humid settings like rain forests [1]. This clay is white or pink and is made up of delicate, microscopic crystals of minerals like silica, quartz, and feldspar. Kaolin is a versatile industrial mineral that is employed in a wide range of applications. The main mineral in kaolin is kaolinite, which has the chemical formula $A1_2O_3$•$2SiO_2$•$2H_2O$ [2, 3]. The kaolin layer comprises a single alumina octahedral sheet and a single silica tetrahedral sheet. The kaolinite structure becomes disordered when Al or Si atoms are substituted. To obtain kaolin with almost perfect composition and minimal accessory mineral impurities, careful processing technology selection is required [4]. Copper, selenium, manganese, magnesium, and zinc are also found naturally in it. It's not commonly consumed for its nutrient value; instead, it's used to treat gastrointestinal issues or applied topically to the skin. Kaolinite and kaolin-pectin are also used in the production of toothpaste, cosmetics, light bulbs, China dishware, porcelain, some types of paper, rubber, paint and a variety of other industrial items [5].

Iron impurity in kaolin clay reduces its economic value by giving undesired colours to the finished items. The most common impurities found in commercial kaolin include biotite, feldspar, muscovite, quartz,

* Corresponding author
E-mail address: ochidanielokey@gmail.com
https://doi.org/10.37121/jase.v6i1.181
2636–607X /2736–0652 © 2022 the authors. Published by **Sciengtex**. This is an open access article under CC BY-NC-ND license (http://creativecommons.org/licenses/by-nc-nd/4.0/)

titanium oxides, and iron oxides or hydroxides, such as magnetite, hematite, and goethite [6]. The mineral's origin and depositional environment determine the presence and degree of these impurities. The kaolin's colour, brightness, and refractoriness are all affected by the presence of iron oxides in the clay. As a result, its commercial price drops significantly [7]. Clay deposits can be coloured red to yellow with as little as 0.4 per cent ferric iron oxides, hydrated oxides and hydroxides. There could be hematite (red), maghemite (reddish-brown), ferrihydrite (brownish red), lepidocrocite (orange), goethite (brownish yellow), and various iron oxide/hydroxides. Similarly, clays like kaolin can be found in iron ores like hematite, presenting problems with blast furnace operation. Therefore, the leaching to make these raw materials commercially valuable is to effectively eliminate iron oxides from kaolinite clays and vice versa [8, 9].

The iron removal processes can be achieved by magnetic separation, sieving or leaching with different chemicals such as oxalic acid and other organic acids in the presence of a fermented medium [10, 11]. In comparison to other organic acids such as citric, malonic, and acetic acid, oxalic acid was selected as a leaching reagent since it has been described to be the best for removing iron from kaolin. This is because oxalic acid has a stronger acidity, complexing power, and may have better reduction ability. An oxalic acid had been used to uncover parameters that could influence the iron dissolution process from kaolin with low iron concentrations [12].

The response surface methodology (RSM) is a collection of statistical and mathematical optimization tools that can be employed to develop, enhance, and optimize processes [13]. When statistical experimental design techniques are applied to the leaching, process variability can be decreased. It's also coupled with the need for fewer resources (time, raw materials and experimental runs). The application of response surface methodology involves three steps: the creation of an experiment plan, the formulation of a model equation, and the analysis and optimization of parameters. This process helps in developing mathematical models used to explain the experimental data taken at some particular blends of the input variables [14].

This research is intended to encourage the fact that clean kaolin is a unique industrial mineral and a functional constituent in a wide range of industrial applications and the necessity to meet Nigeria's kaolin industrial requirements. The annual industrial needs for kaolinites in Nigeria are expected to be more than 360,000 metric tons, whereas the current domestic output is only 110,000 metric tons, resulting in a supply shortfall of over 250,000 metric tons [15]. The goal of this research is to figure out what is the best way to extract iron oxides. The specific objective is the determination of the optimum extraction of iron oxides.

.

2. Materials and Method

The kaolin clay sample from Ibute-Nze in Udi, Enugu State of Nigeria with Global Positioning System (GPS) Device, (Model; Etrex German) 6^{o} 39’ 0” North, 7^{o} 18’ 0” East and altitude 336.00m, was taken from the mine and cleaned of any dirt. The kaolin sample was sun-dried for four days before being pulverized in a mortar and filtered with a 75-micron sieve. The sieved sample was calcined in a furnace that ranged from 200 to 1200 degrees Celsius. The sample was calcined at a temperature of 750 degrees Celsius. In addition, the calcination duration was changed from 30 to 300 minutes. Acids dissolution method, followed by Atomic Absorption Spectroscopy (AAS) to determine the different elements. After 30 minutes of heating at 1000^{o}C, the Loss on ignition (LOI) was determined [16].

2.1. Dissolution Experiment

The leaching experiments were performed using a round bottom reactor (500 mL) with mechanical stirring and constant temperature. Then, the calcined samples were pulverized and sieved into different particle sizes and labelled appropriately. In the 500ml round bottom flask, 1g of the sized portions was weighed out and reacted with a previously calculated volume of the acids for each experiment. The temperature was controlled with a thermo-regulator. In the leaching tests at 85^{o}C, the reactor equipped with a thermometer and a reflux condenser to prevent losses by evaporation was heated with a thermostatically regulated heating mantle. All leaching tests were conducted in one atmosphere for 120 minutes [17]. At the end of the reaction time, the suspension was sieved to remove any undissolved components and washed three times with distilled water. Using an atomic absorption spectrophotometer, the resultant solutions were diluted and tested for iron oxides. The residue was also collected, washed with distilled water to a pH of 7 and then oven-dried at 65^{o}C for 60 min before being reweighed. The weight difference was recorded to determine the amount of iron oxide contaminant that dissolved [18].

2.2. Characterization of the Raw and Calcined Ibute-Nze Kaolin Clay

The ASTM D7263-09 [19] techniques were used to evaluate the raw and calcined clay's physical properties. Chemical analysis of kaolin was carried out using X-ray fluorescence spectroscopy that was controlled by a computer running the Mini-Pal analytical software. The mineral composition of the clay was determined using a PW 4030 x-ray spectrometer with a voltage of 30 kV at 1 mA on a Mini-Pal 4 edition. As a result, the size and morphology of the clay samples were ascertained with scanning electron microscopy (SEM). The SEM micrograph was captured with a JOEL JSM 6400 scanning electron microscope 320x magnification scanning electron microscope recorded at 15 kV [20].

2.3. Design of Experiment (DOE)

A response surface (statistical) study and optimization were carried out using a statistical toolbox of design expert (version 10.0) software for analysis of variance, statistical modelling, surface response study, and optimization. The response surface methodology as an optimization scheme was used for developing empirical models for leaching. The optimization tool's goal is to create a regression-based model and optimize an output response (variable) that is influenced by a set of independent input factors. A series of experiments were carried out in which all of the input variables were changed to determine the cause of the output or response variable change. This method is extremely suitable for a quadratic (second-order polynomial) surface fitting, as it optimizes the independent system variables with less experimental data set [21]. In this paper, an attempt is made to analyse the effect of operating parameters for iron oxide impurities removal of Ibute-Nze kaolin sample in oxalic acid using the response surface methodology by the Box-Behnken design (BBD) method. Consequently, this method was used to study and optimize the removal efficiency of iron oxide by using leaching.

The design of an experiment as a statistical tool is an effective procedure for planning experiments and analysing data obtained for objective conclusions [22]. A Box-Behnken star points giving a total of 46 experiments was used to examine the combined effect of the independent variables (five different factors) leaching temperature, acid concentration, solid to liquid ratio, particle size and time on iron oxide removal, and derive a model. Table 1 shows the factor levels with their corresponding real values. There are five levels of variation in the matrix for the five variables. The process variables are particle size (0.075 – 0.355 mm), reaction temperature (40 – 90 ℃), acid concentration (1 – 6 mol/dm^3), solid-to-liquid ratio (0.02 – 0.12 g/dm^3) and the reaction time (30 – 240 min). The response variable was chosen as the % conversion of iron oxide impurity whereas factor levels were coded as - 1, 0 and +1. These experimental data (factors and response) were fitted into a response surface model for a liquid-solid pair to perform the optimization, as equation (1).

$$Y = \beta_o + \sum_{i=1}^{n} \beta_i x_i + \sum_{i=1}^{n} \beta_{ii} x_i^2 + \sum_{i=1}^{n-1} \sum_{j=i+1}^{n} \beta_{ij} x_i x_j \quad (1)$$

Where, Y is the response, β_o is the constant coefficient, β_i is the linear coefficient, β_{ii} is the quadratic coefficients, and β_{ij} is the interaction coefficients, whereas x_i and x_j are the coded values of the independent process variables [23].

3. Results and Discussion

3.1. Characterization

The results of the chemical compositions of the kaolin are presented in Table 2. The chemical analysis shows the result of the kaolin used. It presents that the Ibute-Nze kaolin sample has 46.64% of SiO_2, 33.10% of Al_2O_3, and 6.45% of iron oxide impurity content, and other trace oxides e.g., calcium oxide, potassium oxide, magnesium oxide, and others when thermally treated at 750^{o}C. Table 2 shows that both raw and calcined Ibute-Nze clay contain the majority of the essential metals. The thermal treatment of Ibute-Nze kaolin specimens causes radical changes in their mineralogical and physical properties.

The iron in the clay is oxidized when it is heated to high temperatures from green/blue Fe^{2+} to reddish-brown Fe^{3+}, which might change the colour of the clay to pink. The brightness of samples has been observed to vary with the calcination temperature, first declining and then improving as the temperature is raised. The conversion of residual surface iron impurities to the highly coloured red iron oxide, hematite, causes the rise in light absorption (brightness reduction) as the calcination temperature approaches 700°C. Heating above 700°C causes a decrease in light absorption, which is mostly due to one or more solid-state processes involving auxiliary components.

After thermal activation, the percentage content of essential metals in the raw clay increased, which could be due to the clay's increased surface area that drew out the metals and made them easier to leach process [24]. Table 3 shows the composition of Ibute-Nze kaolin compared with some clay materials from other locations.

3.2. Physico-Chemical Characterization of the Clay Samples

Table 4 shows the physicochemical parameters of raw and calcined clay. Except for moisture content and bulk density, most properties increased upon calcination, according to the table. After calcination, the porosity increased due to an increase in bulk density [25], allowing the leaching solvent to easily access the clay and improve the leaching process.

Table 1 Experimental range of independent variables with different levels, to study iron oxide impurity removal during the dissolution of Ibute-Nze kaolin in oxalic acid.

Independent variables	Symbols	Range of variables		
		-1	0	+1
Leaching temperature (℃)	A	40	65	90
Particle size (mm)	B	0.075	0.215	0.355
Acid concentration(mol/dm^3)	C	1	3.5	6
Solid-Liquid ratio (g/cm^3)	D	0.02	0.07	0.12
Time (min)	E	30	135	240

Table 2 Chemical composition of Ibute-Nze kaolin clay.

Component	Composition of raw clay (%)	Composition of calcined clay (%)
SiO_2	45.98	46.64
Al_2O_3	32.49	33.10
Fe_2O_3	6.03	6.45
CaO	1.06	1.17
MgO	0.41	0.46
Na_2O	0.17	0.18
TiO_2	3.54	2.20
K_2O	1.35	1.57
LOI	8.97	8.23

Table 3 Chemical composition of Ibute-Nze kaolin clay compared with clay materials from other locations.

Oxides (%)	Ibute-Nze kaolin (Present work)	Okija kaolin [23]	Agbaja kaolin [24]
SiO_2	46.64	47.06	42.00
Al_2O_3	33.10	38.87	35.00
Fe_2O_3	6.45	6.02	13.00
CaO	1.17	0.394	0.72
MgO	0.46	2.045	-
Na_2O	0.18	0.490	-
K_2O	1.57	1.124	5.20
TiO_2	2.20	1.69	2.00

Table 4 Physico-chemical characterization of the clay samples.

Sample	Raw clay	Calcined clay
Moisture content (%)	8.73	4.20
pH	6.42	7.81
Bulk density (g/cm^3)	1.57	1.35
Colour	Greenish-brown	Reddish-brown
Surface area (cm^2/g)	775.68	839.55
Loss on Ignition (%)	9.23	10.97
Total porosity (%)	24.05	49.63
Electrical conductivity (μS/cm)	517.22	559.68

3.3. SEM Results for Raw and Calcined Ibute-Nze Clay Samples

SEM images of the solid sample's morphology are shown in Figs. 1 and 2. The pores are more open after the calcination of the clay, as seen in Fig. 2.

3.4. Statistical Analysis

Table 4 presents the combined effect of the process parameters on the experimental iron oxide leaching efficiency. In general, iron oxide extraction increases to the reasonable point with rising leaching temperature, acid concentration, and time, while decreasing with rising solid-to-liquid ratio and particle size. The data from the leaching experiments were statistically analysed to determine the most significant interaction and quadratic effects. To develop a quadratic response surface model for iron oxide leaching, the data was subjected to multi-regression analysis [26].

For the given levels of each factor, the coded factors equation can be used to make predictions about the response. By comparing the factor coefficients, the coded equation can be utilized to establish the relative impacts of the factors. The final quadratic model (second-order polynomial predictive equation) developed for the analysis of Fe_2O_3 leaching from Ibute-Nze clay at the 95% confidence level is presented in equation (2). The model equation having only the significant coefficients is shown in equation (3) with significant model terms. Then in terms of the actual factors, the model equation (4) is given.

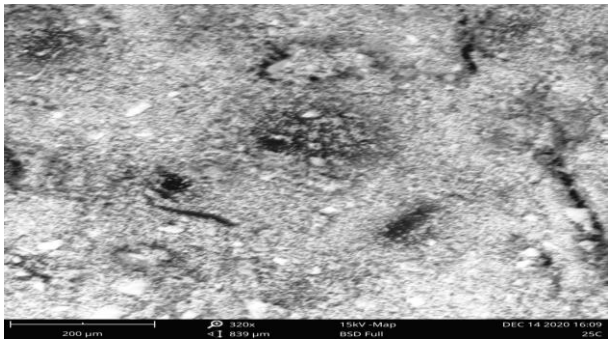

Fig. 1 SEM of a raw Ibute-Nze clay.

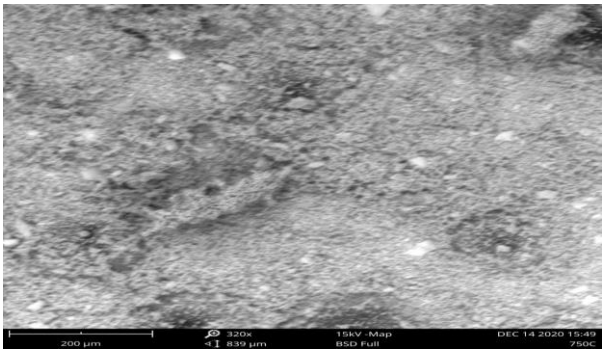

Fig. 2 SEM of a calcined Ibute-Nze clay at 750°C.

Table 4 Experimental design for iron oxide impurity removal from Ibute-Nze kaolin clay.

Run	Leaching temp. (℃), A		Particle size (mm), B		Acid conc. (mol/dm^3), C		Solid/Liquid ratio (g/cm^3), D		Time (min), E		Removal (%)	
	Coded	Real	Coded	Real	Coded	Real	Coded	Real	Coded	Real	Pred	Exp.
1	0.000	65	0.000	0.355	0.000	3.5	0.000	0.07	1.000	240	74.56	75.5453
2	1.000	90	1.000	0.075	0.000	3.5	0.000	0.07	0.000	135	81.80	81.6958
3	-1.000	40	-1.000	0.215	0.000	3.5	0.000	0.07	1.000	240	75.82	75.3115
4	1.000	90	1.000	0.215	1.000	6	0.000	0.07	0.000	135	81.16	82.4157
5	-1.000	40	-1.000	0.215	0.000	3.5	1.000	0.12	0.000	135	75.38	75.8151
6	0.000	65	0.000	0.215	0.000	3.5	0.000	0.07	0.000	135	80.22	80.2154
7	0.000	65	0.000	0.215	0.000	3.5	0.000	0.07	0.000	135	80.22	80.2154
8	1.000	90	1.000	0.215	0.000	3.5	-1.000	0.02	0.000	135	82.88	83.501
9	0.000	65	0.000	0.355	1.000	6	0.000	0.07	0.000	135	80.19	78.6351
10	0.000	65	0.000	0.215	1.000	6	0.000	0.07	-1.000	30	69.34	70.9014
11	0.000	65	0.000	0.215	0.000	3.5	1.000	0.12	1.000	240	75.88	75.8916
12	0.000	65	0.000	0.215	0.000	3.5	0.000	0.07	0.000	135	80.22	80.2154
13	0.000	65	0.000	0.075	0.000	3.5	1.000	0.12	0.000	135	70.26	70.2894
14	0.000	65	0.000	0.215	-1.000	1	-1.000	0.02	0.000	135	74.45	74.6172
15	-1.000	40	-1.000	0.215	0.000	3.5	0.000	0.07	-1.000	30	74.27	69.4416
16	0.000	65	0.000	0.075	0.000	3.5	-1.000	0.02	0.000	135	83.89	83.5501
17	-1.000	40	-1.000	0.355	0.000	3.5	0.000	0.07	0.000	135	74.47	74.601
18	-1.000	40	-1.000	0.215	1.000	6	0.000	0.07	0.000	135	78.42	80.7341
19	-1.000	40	-1.000	0.075	0.000	3.5	0.000	0.07	0.000	135	75.60	75.6817
20	0.000	65	0.000	0.215	0.000	3.5	0.000	0.07	0.000	135	80.22	80.2154
21	0.000	65	0.000	0.215	0.000	3.5	-1.000	0.02	1.000	240	83.95	82.6358
22	0.000	65	0.000	0.215	1.000	6	-1.000	0.02	0.000	135	81.82	80.6186
23	1.000	90	1.000	0.355	0.000	3.5	0.000	0.07	0.000	135	78.02	77.9689
24	0.000	65	0.000	0.215	0.000	3.5	-1.000	0.02	-1.000	30	70.39	70.188
25	0.000	65	0.000	0.215	1.000	6	0.000	0.07	1.000	240	84.62	83.515
26	0.000	65	0.000	0.075	-1.000	1	0.000	0.07	0.000	135	79.97	80.4556
27	1.000	90	1.000	0.215	0.000	3.5	1.000	0.12	0.000	135	79.32	77.5981
28	-1.000	40	-1.000	0.215	-1.000	1	0.000	0.07	0.000	135	73.61	73.2122
29	1.000	90	1.000	0.215	-1.000	1	0.000	0.07	0.000	135	80.61	79.148
30	-1.000	40	-1.000	0.215	0.000	3.5	-1.000	0.02	0.000	135	77.07	79.8436
31	0.000	65	0.000	0.215	1.000	6	1.000	0.12	0.000	135	74.51	73.9577
32	1.000	90	1.000	0.215	0.000	3.5	0.000	0.07	1.000	240	87.26	90.1435
33	1.000	90	1.000	0.215	0.000	3.5	0.000	0.07	-1.000	30	72.57	71.1436
34	0.000	65	0.000	0.355	0.000	3.5	-1.000	0.02	0.000	135	70.43	69.9221
35	0.000	65	0.000	0.355	0.000	3.5	0.000	0.07	-1.000	30	72.32	73.8329
36	0.000	65	0.000	0.215	-1.000	1	1.000	0.12	0.000	135	76.52	77.3341
37	0.000	65	0.000	0.215	-1.000	1	0.000	0.07	-1.000	30	73.82	75.5269
38	0.000	65	0.000	0.215	0.000	3.5	0.000	0.07	0.000	135	80.22	80.2154
39	0.000	65	0.000	0.075	0.000	3.5	0.000	0.07	1.000	240	82.89	82.9101
40	0.000	65	0.000	0.075	0.000	3.5	0.000	0.07	-1.000	30	68.90	69.448
41	0.000	65	0.000	0.355	0.000	3.5	1.000	0.12	0.000	135	78.81	78.6664
42	0.000	65	0.000	0.215	0.000	3.5	0.000	0.07	0.000	135	80.22	80.2154
43	0.000	65	0.000	0.215	-1.000	1	0.000	0.07	1.000	240	74.78	73.8167
44	0.000	65	0.000	0.355	-1.000	1	0.000	0.07	0.000	135	68.63	68.2811
45	0.000	65	0.000	0.075	1.000	6	0.000	0.07	0.000	135	73.76	73.0475
46	0.000	65	0.000	0.215	0.000	3.5	1.000	0.12	-1.000	30	73.20	74.3273

$$\%\ Y_{\text{iron oxide impurity}} = +80.22 + 2.44*A - 1.23*B + 1.34*C - 1.31*D + 4.06*E - 0.66*AB - 1.06*AC - 0.47*AD + 3.28*AE + 4.44*BC + 5.50*BD - 2.94*BE - 2.34*CD + 3.58*CE - 2.72*DE + 0.035*A^2 - 2.78*B^2 - 1.80*C^2 - 1.59*D^2 - 2.77*E^2 \quad (2)$$

$$\%Y_{\text{iron oxide impurity}} = +80.22 + 2.44*A - 1.23*B + 1.34*C - 1.31*D + 4.06*E + 3.28*AE + 4.44*BC + 5.50*BD - 2.94*BE - 2.34*CD + 3.58*CE - 2.72*DE - 2.78*B^2 - 1.80*C^2 - 1.59*D^2 - 2.77*E^2 \quad (3)$$

$$\%Y_{\text{iron oxide impurity removal}} = + 68.25354 + 0.047766*\text{Leaching temperature} - 8.02996*\text{Particle size} + 0.40309*\text{Acid concentration} + 53.79731*\text{Solid/Liquid ratio} + 0.056748*\text{Time} + 1.25048E\text{-}003*\text{Leaching temperature}*\text{Time} + 12.68725*\text{Particle size}*\text{Acid conc.} + 785.89302*\text{ Particle size}*\text{Solid/Liquid ratio} - 0.19982*\text{Particle size}*\text{Time} - 18.75572*\text{Acid conc}*\text{Solid/Liquid ratio} + 0.013642*\text{Acid conc}*\text{Time} - 0.51826\ \text{Solid/Liquid ratio}*\text{Time} - 141.59772*\text{Particle size}^2 - 0.28824*\text{Acid conc}^2 - 635.95115*\text{Solid/Liquid ratio}^2 - 2.51365E\text{-}004*\text{Time}^2 \quad (4)$$

Table 5 shows the outcomes of the analysis of variance (ANOVA), which is appropriate for the experimental design performed. The quadratic regression model's ANOVA suggests that it is significant. The model's F-value (16.02) indicated that it was significant. The model F-value was determined as the ratio of the regression's adjusted mean square to the residual's adjusted mean square. An F-value of this magnitude has a 0.01% chance of occurring due to noise. The P-value for the model (Prob.> F) is quite low, indicating that the model is significant. P-values were employed to determine the significance of each model's coefficients as presented (Table 5). The lower the P-value, the more significant the respective coefficients become [27]. The values of $P < 0.05$ imply that the model terms are significant. The values of P for the coefficients estimated (Table 4) specify that among the tested variables used in the design, A, B, C, D, E, AE, BC, BD, BE, CD, CE, DE, B^2, C^2, D^2 and E^2 (where A = leaching temperature, B = particle size, C= acid concentration, D = solid/liquid ratio and E = contact/reaction time) are significant model terms. The R-squared (R^2) as the statistical measure shows the proportion of the variance for a dependent variable, which is represented by an independent variable in a regression model. Furthermore, modified R-squared corrects statistics for the number of independent variables in the model. Any of the equations that best fits the leaching process based on adjusted R-squared (closest positive value to 1) will be chosen as the statistical model that best describes the leaching process and will thus be employed to deduce the optimum leaching conditions. Similarly, R-squared was used as a measure of data variability, but its acceptability was determined by comparing it to the p-value for F-statistics.

Table 5 ANOVA for response surface quadratic model

Source	Sum of squares	df	Mean square	F value	p-value Prob > F	
Model	956.41	20	47.82	16.02	< 0.0001	significant
A-Leaching Temperature	94.93	1	94.93	31.81	< 0.0001	
B-Particle size	24.07	1	24.07	8.06	0.0088	
C-Acid Concentration	28.71	1	28.71	9.62	0.0047	
D-Solid/Liquid Ratio	27.55	1	27.55	9.23	0.0055	
E-Time	263.73	1	263.73	88.36	< 0.0001	
AB	1.75	1	1.75	0.59	0.4510	
AC	4.52	1	4.52	1.52	0.2297	
AD	0.88	1	0.88	0.29	0.5923	
AE	43.10	1	43.10	14.44	0.0008	
BC	78.87	1	78.87	26.42	< 0.0001	
BD	121.06	1	121.06	40.56	< 0.0001	
BE	34.51	1	34.51	11.56	0.0023	
CD	21.99	1	21.99	7.37	0.0119	
CE	51.29	1	51.29	17.18	0.0003	
DE	29.61	1	29.61	9.92	0.0042	
A^2	0.011	1	0.011	3.593E-003	0.9527	
B^2	67.22	1	67.22	22.52	< 0.0001	
C^2	28.32	1	28.32	9.49	0.0050	
D^2	22.06	1	22.06	7.39	0.0117	
E^2	67.03	1	67.03	22.46	< 0.0001	
Residual	74.62	25	2.98			
Lack of Fit	74.62	20	3.73			
Pure Error	0.000	5	0.000			
Cor Total	1031.03	45				

Std. Dev. = 1.73, Mean = 77.12, C.V. % = 2.24, PRESS = 298.49, -2Log Likelihood = 152.80, R-Squared = 0.9276, Adj. R-Squared = 0.8697, Pred R-Square = 0.7105, Adeq. Precision = 15.956, BIC = 233.20 and AICc = 233.30

The adequacy of the model for these data was determined using the p-value of F-statistics, with a p-value ≤ 0.05 considered acceptable based on 95 per cent confidence intervals. The significance of the major effects was obtained by using ANOVA, assessed in the same way with F-statistics via the p-value whereas the statistical significance of each factor or their interactions in the model was determined by either the t-statistics value or its associated p-value in the process. Statistical interaction between factors was determined using the contour lines and corroborated with the numerical values from t-statistics of surface plots. The coefficient of regression (R^2) was found to be 0.9276, indicating that the regression model accounts for 92.76 per cent of the variability in the yield data, indicating a very good fit. A better fitting model is indicated by the adjusted R-squared, R-Sq (adj.) value of 0.8697. This index is a measure of how well a model fits the data [28].

Two separate tests (sequential model sum of squares and model summary statistics) were used to determine the adequacy of the models showing the elimination of iron oxide impurity by the dissolution of the kaolin sample in hydrochloric acid. Table 6 summarizes the corresponding outcomes. The sequential model's results revealed that the 2FI model did not adequately describe the experimental data. The "Predicted R^2" of 0.7105 for the quadratic model was in reasonable agreement with the "Adjusted R^2" of 0.8697, as seen in the model summary statistics. The quadratic model also had the highest significant "Predicted R^2" and "Adjusted R^2" values. The given findings suggest that the quadratic model explained the interaction between the independent factors and the matching response excellently [29].

The Akaike information criterion (AIC) is a mathematical method for determining how well a model fits the data from which it was built. AIC is a statistical method for comparing several models and determining which one is the best fit for the data. The best fit for the data can be determined by calculating and comparing the AIC scores of various different models. Using the highest likelihood estimate and the number of parameters (independent variables) in the model, AIC calculates the relative information value of the model. The model's information score (the lower-case 'c' indicates that the value was derived using the AIC test with small sample sizes corrected). The value of AICc (233.30) implies that the model is good. The lower the AIC value, the better model fits [30].

As indicated in Fig. 3, the data were also evaluated to see if there was a correlation between the experimental and calculated iron oxide impurity removal (Y per cent). The observed response data for the design runs using the BBD technique served as the experimental values, while the quadratic equation was used for the predicted values. Fig. 3 indicates that the data points on the plot were fairly scattered near the straight line ($R^2 = 0.9971$), showing a strong correlation between the experimental and computed response values and that the preceding analysis' underlying assumptions were correct [25]. Fig. 4 shows the normal probability plot that presents the residuals following a normal distribution, in which case the points follow a straight-line arrangement.

Table 6 Adequacy of the model tested.

Source	Sum of Squares	Degree of Freedom	Mean Square	F Value	p-value Prob > F	
Sequential Model Sum of Squares						
Mean vs Total	2.736E+005	1	2.736E+005			
Linear vs Mean	439.01	5	87.80	5.93	0.0003	
2FI vs Linear	387.59	10	38.76	5.69	< 0.0001	
Quadratic vs 2FI	129.82	5	25.96	8.70	< 0.0001	Suggested
Cubic vs Quadratic	64.76	15	4.32	4.38	0.0116	Aliased
Residual	9.87	10	0.99			
Total	2.746E+005	46	5969.71			
Lack of Fit Tests						
Source	Sum of Squares	Degree of Freedom	Mean Square	F Value	p-value Prob > F	
Linear	592.03	35	16.92			
2FI	204.44	25	8.18			
Quadratic	74.62	20	3.73			
Cubic	9.87	5	1.97			
Pure Error	0.000	5	0.000			
Model Summary Statistics						
Source	Std. Dev.	R-Squared	Adjusted R-Squared	Predicted R-Squared	PRESS	
Linear	3.85	0.4258	0.3540	0.2296	794.26	
2FI	2.61	0.8017	0.7026	0.5502	463.79	
Quadratic	1.73	0.9276	0.8697	0.7105	298.49	Suggested
Cubic	0.99	0.9904	0.9569	0.3876	631.42	Aliased

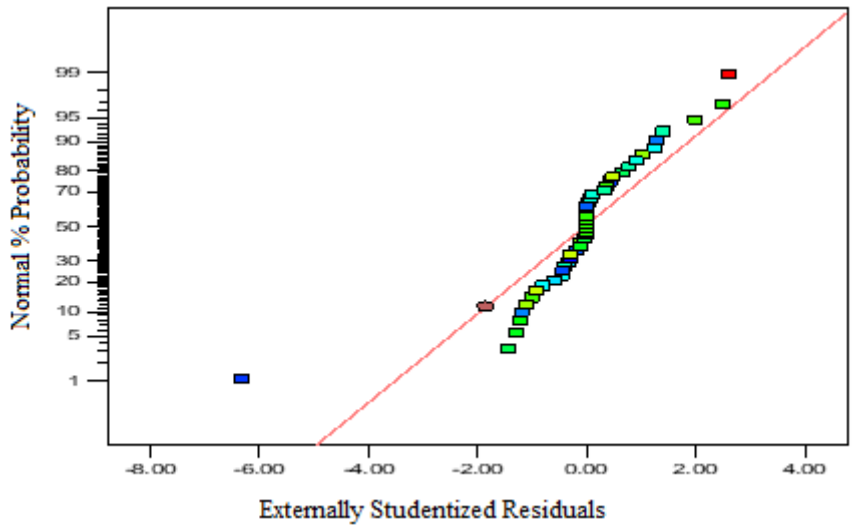

Fig. 3 Plot of normal probability against residuals.

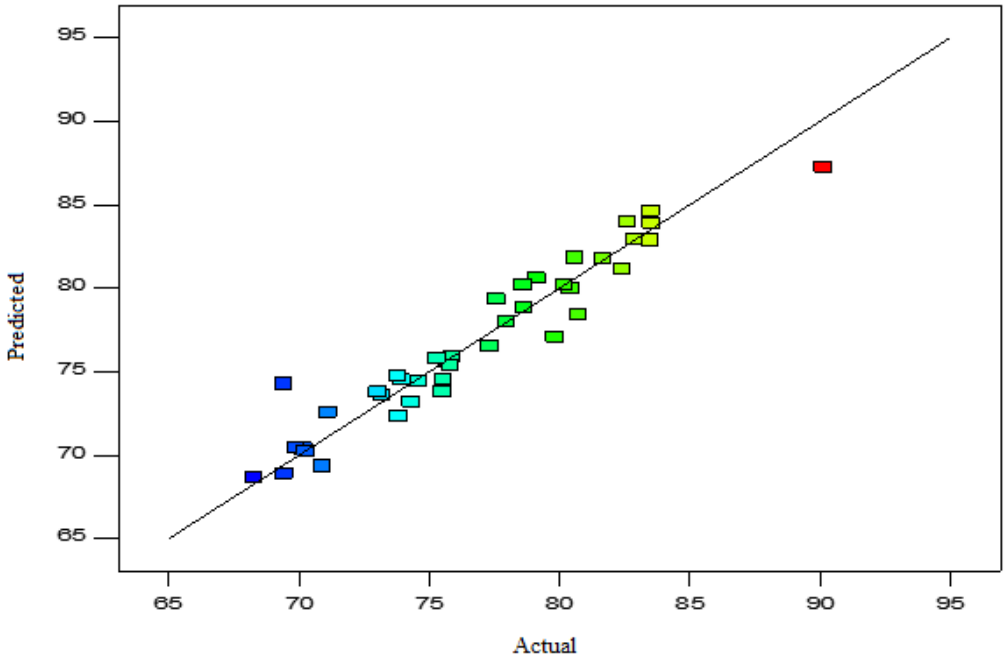

Fig. 4 Predicted values against the experimental values.

The residuals are plotted against the experimental run order in Fig. 5. It enables you to look for input variables that could have influenced the result of the experiment. A random scatter should be seen on the plot. Trends imply the presence of a time-related variable in the background. Blocking and randomization protect the analysis from being ruined by trends [31].

3.5. Three-Dimensional (3D) Response Surface Plots

The 3D response surface plots, shown in Figs. 6(a)-(j), are useful in understanding the major influence and interactions of the five considered variables. The corresponding contour plots allow for a clear assessment of the independent factors' impacts on the dependent variable. The optimization outcome of the leaching temperature, Figs. 6(a)-(d), showed that increasing the leaching temperature increased iron oxide removal up to 85.15^{o}C, but further increases had no significant improvement in iron oxide removal. The iron dissolution increased as the acid concentration increased (Figs. 6(b), (e), (h), and (i)). The optimum iron oxide removal was obtained at an acid concentration of 3.89 mol/dm^3, whereas increasing the acid concentration further did not cause a significant rise in the iron removal. The optimization result of time (Figs. 6 (d), (g), (i), and (j)) showed a rise in iron removal with increasing time up to the optimal value of 220 min, after which further increases had no significant effect on the iron removal. The optimization result of the particle size (Figs. 6(a), (e)-(g)) revealed that iron removal increased with a decrease in size of about 0.08mm and remained stable as this increased the surface area. Figs. 6(c), (f), (h), and (j) show that decreasing the clay-acid ratio increased the iron removal. The ratio of 0.03g/cm^3 produced the best results, which is similar to the report of an independent study [27].

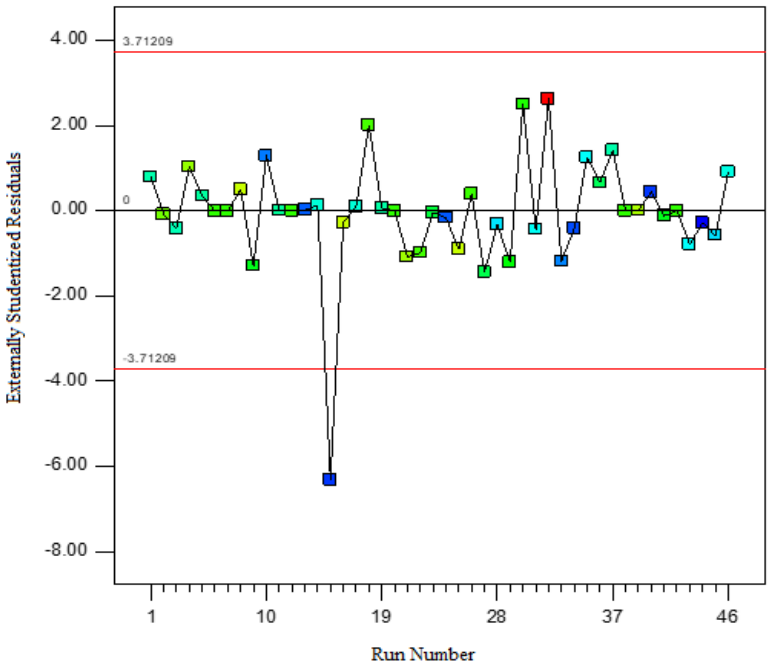

Fig. 5 Plot of residuals against the experimental run order.

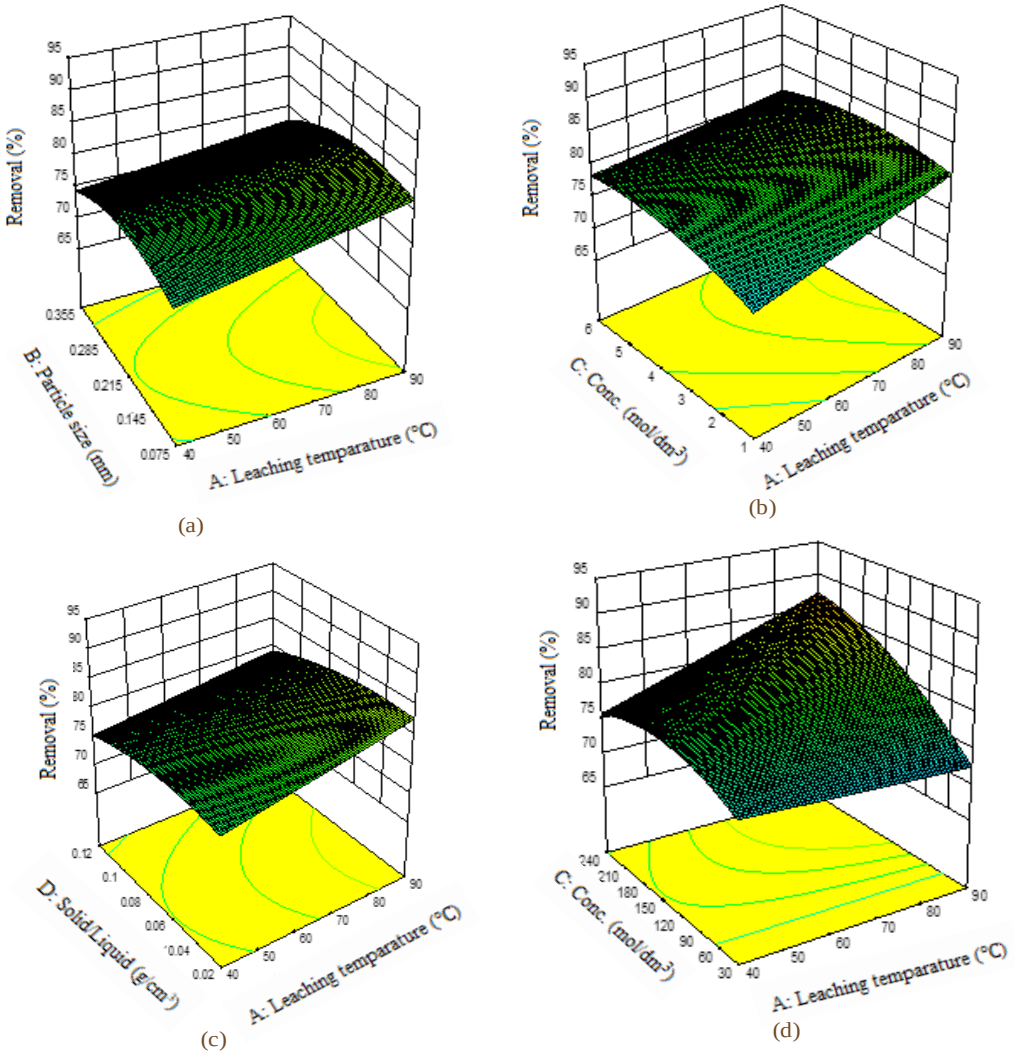

Fig. 6 3D plots for % iron oxide impurity removal versus (a) particle size and leaching temperature, (b) acid concentration and leaching temperature, (c) solid-liquid ratio and leaching temperature, and (d) time and leaching temperature

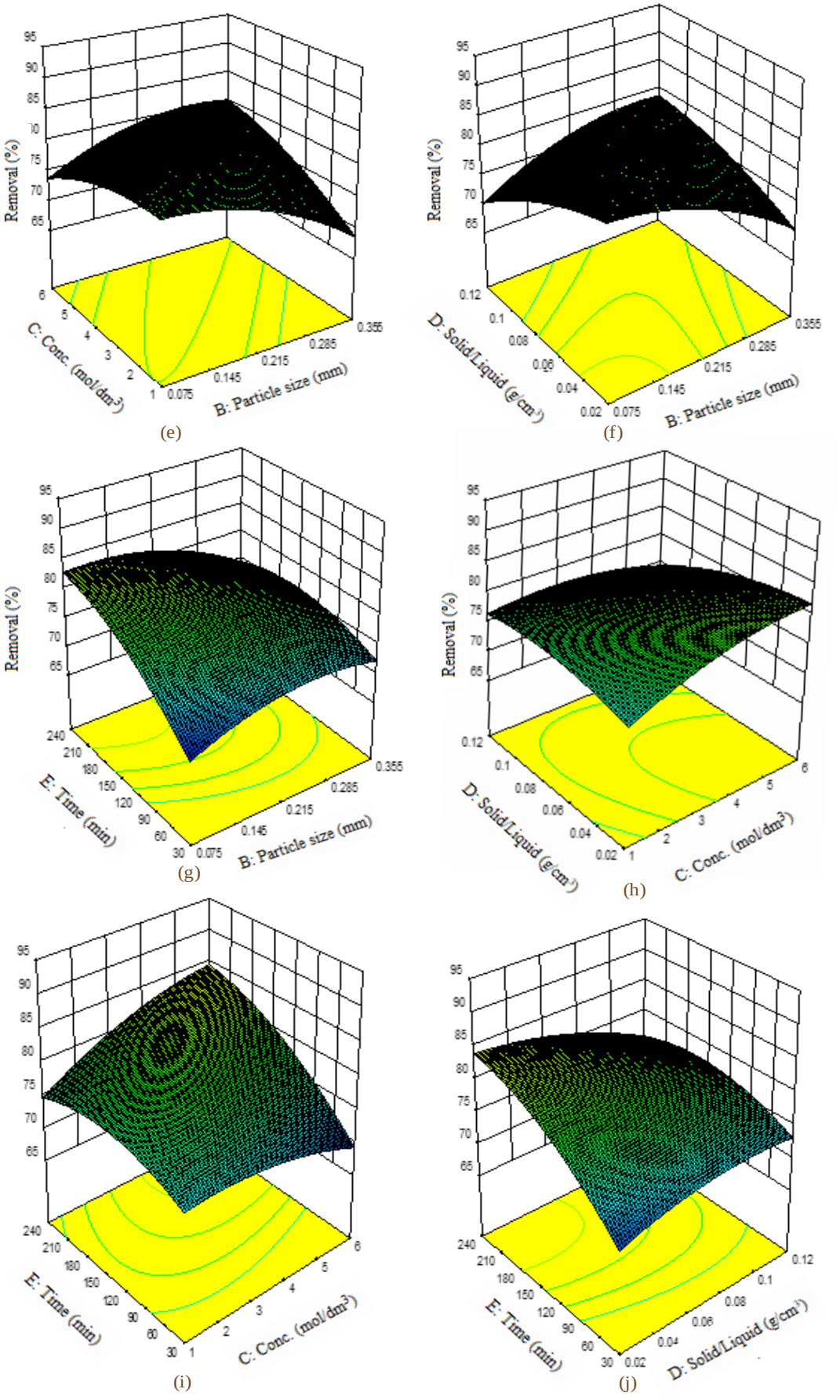

Fig. 6 (cont.) 3D plots for % iron oxide impurity removal versus, (e) acid concentration and particle size, (f) solid-liquid ratio and particle size, (g) time particle and size, (h) solid-liquid ratio and acid concentration, (i) time and acid concentration, and (j) time and solid-liquid ratio.

Table 7 The optimum parameters predicted and experimental result.

Optimum parameters predicted					Removal efficiency	
Leaching Temperature (℃)	Particle size (mm)	Concentration (mol/dm^3)	Solid/liquid (g/cm^3)	Time (min)	Predicted (%)	Experimental (%)
83.2061	0.0827	3.6179	0.0287	217.932	93.0974	92.6035

3.6. Numerical Optimization

A basic objective of this research is to determine the best process parameters for removing iron oxide impurities from Ibute-Nze kaolin in an oxalic acid solution. The optimal values of the process variables, shown in Table 7, were a leaching temperature (83.2061^{o}C), a particle size (0.0827mm), an acid concentration (3.6179mol/dm^3), a solid-liquid ratio (0.0287g/cm^3), and a time of 217.932 min, according to the model capable of predicting the maximum iron oxide impurity removal efficiency. The predicted per cent iron oxide removal efficiency under these conditions was 93.0974 per cent, which was very close to the experimental result of 92.6035 per cent.

4. Conclusion

The leaching process has been shown as a promising method efficient for removing iron impurities from kaolin. The results of response surface methodology revealed that leaching variables like acid concentration, leaching temperature, particle size, solid/liquid ratio, and time have a considerable influence on the dependent variable, per cent removal of iron oxide. The foremost significant parameters among these variables are acid concentration and leaching temperature. Leaching temperature, acid concentration, and time were all positively connected with per cent iron oxide removal, however, the solid/liquid ratio was negatively correlated. The optimal leaching parameters of iron oxide from Ibute-Nze clay are leaching temperature of 83.2061^{o}C, acid concentration (3.6179mol/dm^3), particle size (0.0827mm), solid/liquid ratio (0.0287 g/cm^3), and time of 217.932 min; according to the Box-Behnken design, three-dimensional plots, and contour plots.

Conflict of Interests

The authors declare that there is no conflict of int regarding the publication of this paper.

ORCID

D. O. Ochi https://orcid.org/0000-0002-5678-2174

References

[1] R. A. Hernandez Hernandez, F. Legorreta Garcia, L. E. Hernandez Cruz, A. Martinez Luevanos, “Iron removal from a kaolinitic clay by leaching to obtain high whiteness index,” IOP Conference Series: Materials Science and Engineering, vol. 45, no. 012002, 2013.

[2] U. Udeigwe, O. D. Onukwuli, R. Ajemba, C. N. Ude, “Kinetics studies of hydrochloric acid leaching of alumina from Agbaja clay,” International Journal of Research in Advanced Engineering and Technology, vol. 1, no. 1, pp. 64-72, 2015.

[3] G. Olaremu, “Sequential leaching for the production of alumina from a Nigerian clay,” International Journal of Engineering Technology, Management and Applied Sciences, vol. 3, no. 7, pp. 103-108, 2015.

[4] Schroeder, G. Erickson, “Kaolin: From ancient porcelains to nanocomposites,” Elements, vol. 10, pp. 177-182, 2014.

[5] M. Lu, G. Xia, X. Zhang, "Refinement of industrial kaolin by removal of iron-bearing impurities using thiourea dioxide under mechanical activation,” Applied Clay Science, vol. 141, pp. 192-197, 2017.

[6] M. Gougazeh, “Removal of iron and titanium contaminants from Jordanian kaolins by using chemical leaching,” Journal of Taibah University for Science, vol. 12, no. 3, pp. 247-254, 2018.

[7] K. A. Eze, J. O. Nwadiogbu, E. T. Nwankwere, “Effect of acid treatments on the physicochemical properties of kaolin clay,” Archives of Applied Science Research, vol. 4, pp.792-794, 2012.

[8] R. A. Hernández Hernández, F. Legorreta García, L. E. Hernández Cruz, A. Bedolla Jacuinde, “Kaolin bleaching by leaching using phosphoric acid solutions,” Journal of the Mexican Chemical Society, vol. 59, no. 3, pp. 198-202, 2015.

[9] S. S. Jikan, N. A. Badarulzaman, S., Yahaya, A. D. Adamu, “Delamination of Kaolinite by intercalation of urea using milling,” Materials Science Forum, vol. 888, pp. 136-140, 2017.

[10] Q-X. He, Xi.-C. Huang, Z-L. Chen, " Influence of organic acids, complexing agents and heavy metals on the bioleaching of iron from kaolin using Fe(III)-reducing bacteria," Applied Clay Science, vol. 51, no. 4, pp. 478-483, 2011,

[11] N. Zari, M. Raji, H. El Mghari, R. Bouhfid, A.e.K. Qaiss, "3 - Nanoclay and polymer-based nanocomposites: Materials for energy efficiency," M. Jawaid, M. M. Khan, (eds), in Woodhead Publishing Series in Composites Science and Engineering, Polymer-based Nanocomposites for Energy and Environmental Applications, Woodhead Publishing, pp. 75-103, 2018.

[12] F. Legorreta G., E. Salinas R., L. E. Hernandez C., R. A. Hernandez H., and E. Cerecedo S., "Kinetics study of iron leaching from kaolinitic clay using oxalic acid", European Scientific Journal, *ESJ*, vol. 11, no. 12, pp. 12-23, 2015.

[13] S. Malik, "Optimization of machining parameters of En24 alloy steel on WEDM Using RSM," International Journal of Advanced Research in IT and Engineering, vol. 3, no. 3, pp. 9-20, 2014.

[14] K. Pariyanerest, M. R. Hosseini, A. Ahmadi, A. Zahiri, "Optimization and kinetics of oxalic acid treatment of feldspar for removing the iron oxide impurities," Separation Science and Technology, vol. 55, no. 10, pp. 1871-1882, 2020.

[15] O. A, Talabi, O. L Ademilua, O. O. Akinola, "Compositional features and industrial application of Ikere kaolinite, southwestern Nigeria," Research Journal in Engineering and Applied Sciences, vol. 1, no. 5, pp. 327-333, 2012.

[16] T. M. Ahmed, A. A. Alomari, "Extraction of alumina from Nawan kaolin by acid leaching," Oriental Journal of Chemistry, vol. 35, pp. 1013-1021, 2019.

[17] G. Olaremu, "Physico-chemical characterization of Akoko mined kaolin clay," Journal of Mineral and Materials Characterization and Engineering, vol. 3, no. 5, pp. 353–361, 2015.

[18] H. Wang, Q. Feng, K. Liu, "The dissolution behaviour and mechanism of kaolinite in alkali-acid leaching process," Applied Clay Science, vol. 132, pp. 273–280, 2016.

[19] ASTM D7263-09, "Standard test methods for laboratory determination of density (unit weight) of soil specimens," ASTM International, West Conshohocken, PA, www.astm.org (accessed: October 2017).

[20] M. Gray, M. G. Johnson, M. I. Dragila, M. Kleber, "Water uptake in biochars: The roles of porosity and hydrophobicity," Biomass and Bioenergy, vol. 61, pp. 196-205, 2014.

[21] V. Arslan, "The modelling and optimization of iron removal from silica sand under ultrasound-assisted leaching by response surface methodology," Mining, Metallurgy & Exploration, vol.38, pp. 2229–2237, 2021.

[22] M. Taran, E. Aghaie, "Designing and optimization of the separation process of iron impurities from kaolin by oxalic acid in the bench-scale stirred-tank reactor," Applied Clay Science, vol. 107, pp. 109-116, 2015.

[23] S. Ajana, O. D. Onukwuli, R. O. Ajemba, C. F. Okey-Onyesolu, C. C. Okoye, "Leaching of Okija kaolin iron-oxides impurity with HCl: optimization of dissolution conditions using response surface methodology," Integrated Journal of Engineering Research and Technology, vol. 2, no. 3, pp. 201-214, 2015.

[24] O. D. Onukwuli U. Uchenna, U. C. Nonso, "Process optimization of hydrochloric acid leaching of iron from Agbaja clay," Journal of Chemical Technology and Metallurgy, vol. 53, pp. 581-589, 2018.

[25] M. Onoh, G. O. Mbah, E. R. Mbah-Iroulo, "Optimization and process modelling of the extraction of iron oxide from Aku clay by hydrochloric acid leaching," American Journal of Engineering Research, vol. 7, no. 6, pp-87-98, 2018.

[26] R. Swain, and R. Bhima Rao, "Application of response surface methodology on leaching of iron from partially laterised khondalite rocks: A bauxite mining waste," Journal of the Institution of Engineers (India): Series D, vol. 99, pp. 23-31, 2018.

[27] R. O. Ajemba, O. D. Onukwuli, "Determination of the optimum dissolution optimum dissolution conditions of Ukpor clay in hydrochloric acid using response surface methodology," International Journal of Engineering Research Application, vol. 2, pp. 732-742, 2012.

[28] O. H. Orugba, O. D. Onukwuli, N. C. Njoku, "Process modelling of sulphuric acid leaching of Iron from Ozoro clay," European Scientific Journal, vol. 10, no. 30, 256-268, 2014.

[29] M. Saldaña, N. Toro, J. Castillo, P. Hernández, A. Navarra, "Optimization of the heap leaching process through changes in modes of operation and discrete event simulation," Minerals, vol. 9, no. 421, 2019, https://doi.org/10.3390/min9070421

[30] A. Boisbunon, S. Canu, D. Fourdrinier, W. Strawderman, M. T. Wells, "Akaike's information criterion, C_p and estimators of loss for elliptically symmetric distributions", International Statistical Review," vol. 82, no. 3, pp. 422–439, 2014.

[31] S. O. Egbuna, G. O. Mba, E. R. Mbah-Iroulo, "Optimization and process modelling of the extraction of alumina from Aku clay by hydrochloric acid leaching," American Journal of Engineering Research, vol. 7, no. 11, pp. 158-169, 2018.